

Supporting Information for

Elucidation the two-step relaxation processes of a tetrานuclear dysprosium molecular nanomagnet through magnetic dilution

Yu Fang,^a Xiao-Qin Ji,^a Jin Xiong,^c Guanzheng Li,^{a,d} Fang Ma,^a Hao-Ling Sun,^{*a} Yi-Quan Zhang^{*b} and Song Gao^{*c}

^a Department of Chemistry and Beijing Key Laboratory of Energy Conversion and Storage Materials, Beijing Normal University, Beijing 100875, P. R. China. E-mail: haolingsun@bnu.edu.cn;

^b Jiangsu Key Laboratory for NSLSCS, School of Physical Science and Technology, Nanjing Normal University, Nanjing 210023, P. R. China. E-mail: zhangyiquan@njnu.edu.cn;

^c Beijing National Laboratory for Molecular Sciences, State Key Laboratory of Rare Earth Materials Chemistry and Applications, College of Chemistry and Molecular Engineering, Peking University, Beijing 100871, China. E-mail: gaosong@pku.edu.cn;

^d No 7 Yunhan RD, Shuitu Hi-tech Industrial Zone, Chongqing 400714, P. R. China.

Computational details

There are two types of Dy³⁺ ions for complex **1**, and thus we need to calculate two Dy³⁺ fragments. Complete-active-space self-consistent field (CASSCF) calculations on individual Dy³⁺ fragments of the model structure (see Fig. S11 for the calculated model structure of **Dy1**; another calculated model is similar) extracted from the compound on the basis of single-crystal X-ray determined geometry have been carried out with MOLCAS 8.2¹ program package. Each individual Dy³⁺ fragment was calculated keeping the experimentally determined structure of the corresponding compound while replacing the other Dy³⁺ ions by diamagnetic Lu³⁺.

The basis sets for all atoms are atomic natural orbitals from the MOLCAS ANO-RCC library: ANO-RCC-VTZP for Dy³⁺ ions; VTZ for close N and O; VDZ for distant atoms. The calculations employed the second order Douglas-Kroll-Hess Hamiltonian, where scalar relativistic contractions were taken into account in the basis set and the spin-orbit couplings were handled separately in the restricted active space state interaction (RASSI-SO) procedure. For individual Dy³⁺ fragment, active electrons in 7 active spaces include all *f* electrons (CAS (9 in 7)) in the CASSCF calculation. To exclude all the doubts, we calculated all the roots in the active space. We have mixed the maximum number of spin-free state which was possible with our hardware (all from 21 sextets, 128 from 224 quadruplets, 130 from 490 doublets). Single_Aniso² program was used to obtain the **g** tensors, energy levels, magnetic axes, *et al.*, based on the above CASSCF/RASSI calculations.

Fitting the exchange interaction in complex **1** using Lines model based on CASSCF results

To fit the exchange interactions in complex **1**, we took two steps to obtain them. Firstly, we calculated individual Dy³⁺ fragments using CASSCF/RASSI to obtain the corresponding magnetic properties. Then, the exchange interaction between the magnetic centers is considered within the Lines model,³ while the account of the dipole-dipole magnetic coupling is treated exactly. The Lines model is effective and has been successfully used widely in the research field of *f*-elements single-molecule magnets.⁴

For complex **1**, there are four types of *J* (see Fig. S13).

The exchange Ising Hamiltonian is:

$$\hat{H}_{exch} = -J_1^{total} (\hat{\vec{S}}_{Dy1} \cdot \hat{\vec{S}}_{Dy2} + \hat{\vec{S}}_{Dy1a} \cdot \hat{\vec{S}}_{Dy2a}) - J_2^{total} (\hat{\vec{S}}_{Dy1a} \cdot \hat{\vec{S}}_{Dy2} + \hat{\vec{S}}_{Dy1} \cdot \hat{\vec{S}}_{Dy2a}) - J_3^{total} \hat{\vec{S}}_{Dy2} \cdot \hat{\vec{S}}_{Dy2a} - J_4^{total} \hat{\vec{S}}_{Dy1} \cdot \hat{\vec{S}}_{Dy1a} \quad (S1)$$

The J_1^{total} , J_2^{total} , J_3^{total} and J_4^{total} are the parameters of the total magnetic interaction (

$J^{total} = J^{dipolar} + J^{exchange}$) between magnetic center ions. The $\tilde{S}_{Dy} = \pm 1/2$ are the ground pseudospin on the Dy³⁺ sites. The dipolar magnetic coupling can be calculated exactly, while the exchange coupling constants were fitted through comparison of the computed and measured magnetic susceptibilities using the Poly_Aniso program.²

Table S1. Selected bond distances (\AA) and angles ($^{\circ}$) in complex **1**.

Dy(1)-O(3)	2.209(5)	Dy(1)-O(7)	2.314(5)	Dy(1)-O(10)	2.322(6)
Dy(1)-O(6)	2.394(5)	Dy(1)-O(2)	2.389(5)	Dy(1)-O(9)	2.433(5)
Dy(1)-O(8)	2.451(6)	Dy(1)-N(4)	2.543(7)	Dy(2)-O(1)	2.169(6)
Dy(2)-O(11)	2.349(5)	Dy(2)-O(12)	2.375(5)	Dy(2)-O(2)	2.399(5)
Dy(2)-O(4)	2.423(5)	Dy(2)-O(6)	2.403(5)	Dy(2)-O(5)	2.460(5)
Dy(2)-N(1)	2.515(7)				
Dy(1)-O(2)-Dy(2)		112.5(2)		Dy(1)-O(6)-Dy(2)	112.2(2)

Symmetry code: a = -x+1,-y,-z+2

Table S2. Hydrogen bonds in **1**.

D-H	d(D-H) (\AA)	\angle DHA ($^{\circ}$)	d(D...A) (\AA)	A
N2-H2	0.880	150.60	1.882	O9 [1-x, -y, 1-z]

Table S3. Relaxation fitting parameters for Cole-Cole plots of using the sum of two modified Debye functions under zero dc field of complex **1**.

eq.1							
T/K	χ_s	χ_t	β	τ_1	α_1	τ_2	α_2
2	0.00	30.39	0.56	9.71E-03	0.23	6.05E-04	0.43
2.5	0.05	24.33	0.55	8.28E-03	0.25	3.66E-04	0.42
3	0.06	20.09	0.50	7.76E-03	0.23	2.97E-04	0.42
3.5	0.04	17.03	0.47	7.39E-03	0.22	2.45E-04	0.43
4	0.05	14.73	0.44	7.07E-03	0.21	2.03E-04	0.43
4.5	0.13	12.94	0.44	6.59E-03	0.21	1.58E-04	0.43
5	0.12	11.53	0.43	6.18E-03	0.20	1.24E-04	0.44
5.5	0.07	10.39	0.41	5.76E-03	0.18	9.05E-05	0.46
6	0.01	9.48	0.39	5.19E-03	0.17	6.77E-05	0.50
6.5	0.01	8.72	0.34	4.60E-03	0.14	4.56E-05	0.56
7	0.02	8.08	0.33	3.89E-03	0.13	2.63E-05	0.59
7.5	0.03	7.52	0.36	3.33E-03	0.13	1.99E-05	0.61
eq.2							
T/K	χ_T	χ_s	α	$\tau''(s)$			
7.5	7.43	3.34	0.22	2.56E-03			
8	6.94	3.05	0.23	2.09E-03			
8.5	6.51	2.98	0.21	1.86E-03			
9	6.12	2.72	0.23	1.44E-03			
9.5	5.79	2.63	0.22	1.22E-03			
10	5.47	2.52	0.21	1.01E-03			
10.5	5.20	2.45	0.20	8.43E-04			
11	4.96	2.34	0.21	6.50E-04			
11.5	4.75	2.23	0.22	5.17E-04			
12	4.52	2.18	0.19	3.91E-04			
12.5	4.29	2.13	0.16	2.81E-04			
13	4.14	2.02	0.18	2.11E-04			
13.5	3.96	1.99	0.19	1.49E-04			
14	3.79	1.90	0.21	1.03E-04			
14.5	3.61	1.90	0.22	7.15E-05			
15	3.30	1.65	0.20	5.10E-05			
15.5	3.20	1.56	0.28	3.20E-05			
16	3.10	1.48	0.31	2.08E-05			

Table S4. Relaxation fitting parameters from Least-Squares Fitting of $\chi(f)$ data under zero dc field of complex **3**.

T	χ_T	χ_s	α	$\tau''(s)$
2	27.577	3.825	0.562	2.976E-4
2.5	21.882	3.815	0.537	3.133E-4
3	18.219	3.498	0.523	2.961E-4
3.5	15.564	3.519	0.501	2.894E-4
4	13.574	3.448	0.482	2.653E-4
4.5	11.992	3.526	0.457	2.443E-4
5	10.753	3.609	0.438	2.213E-4
5.5	9.780	3.444	0.440	1.775E-4
6	8.970	3.390	0.443	1.460E-4
6.5	8.297	3.317	0.458	1.191E-4
7	7.714	3.380	0.467	1.049E-4
7.5	7.229	3.340	0.489	9.005E-5
12.5	4.304	2.498	0.460	7.325E-5
13	4.104	2.488	0.423	6.979E-5
13.5	3.914	2.466	0.362	6.580E-5
14	3.774	2.375	0.389	5.544E-5
14.5	3.595	2.356	0.340	4.862E-5
15	3.494	2.247	0.374	3.859E-5
15.5	3.367	2.175	0.376	3.022E-5
16	3.264	2.089	0.395	2.254E-5
16.5	3.179	2.001	0.434	1.622E-5
17	3.086	1.920	0.458	1.169E-5
17.5	3.005	1.834	0.494	8.265E-6
18	2.945	1.757	0.544	5.825E-6

Table S5. Calculated energy levels (cm^{-1}), \mathbf{g} (g_x , g_y , g_z) tensors and m_J values of the lowest eight Kramers doublets (KDs) of individual Dy^{3+} fragments of complex **1** using CASSCF/RASSI with MOLCAS 8.2.

KDs	Dy1(Dy1a)			Dy2(Dy2a)		
	E/cm^{-1}	\mathbf{g}	m_J	E/cm^{-1}	\mathbf{g}	m_J
1	0.0	0.018			0.071	
		0.243	$\pm 15/2$	0.0	0.201	$\pm 15/2$
		19.184			19.487	
2	39.3	0.027			0.129	
		0.283	$\pm 3/2$	57.0	0.334	$\pm 1/2$
		18.866			19.344	
3	130.8	1.622			1.430	
		4.469	$\pm 9/2$	160.6	1.582	$\pm 13/2$
		12.916			15.771	
4	159.1	10.567			1.011	
		6.767	$\pm 7/2$	215.9	4.437	$\pm 3/2$
		1.269			13.290	
5	215.2	2.374			3.292	
		3.329	$\pm 5/2$	263.0	5.847	$\pm 5/2$
		8.310			12.252	
6	256.9	0.040			2.289	
		5.359	$\pm 11/2$	335.8	4.123	$\pm 7/2$
		10.974			8.773	
7	291.8	2.646			1.571	
		3.427	$\pm 1/2$	373.4	3.453	$\pm 9/2$
		11.733			8.677	
8	355.0	0.498			0.460	
		1.063	$\pm 13/2$	417.4	2.440	$\pm 11/2$
		17.438			16.098	

Table S6. Fitted exchange coupling constant J_{exch} , the calculated dipole-dipole interaction J_{dip} and the total J between Dy^{3+} ions in complex **1** (cm^{-1}). The intermolecular interactions zJ' of complex **1** was fitted to 0.005 cm^{-1} .

	J_1	J_2	J_3	J_4
J_{dip}	-0.06	1.52	0.64	0.26
J_{exch}	-5.75	-8.25	-0.50	0.75
J_{total}	-5.81	-6.73	0.14	1.11

Table S7. Exchange energies (cm^{-1}) and main values of the g_z for the lowest eight exchange doublets of complex **1**.

	1	
	Energy	g_z
1	0.0	49.010
2	0.4	0.008
3	0.5	35.487
4	0.5	35.448
5	0.9	55.390
6	0.9	38.944
7	0.9	39.986
8	1.6	0.000

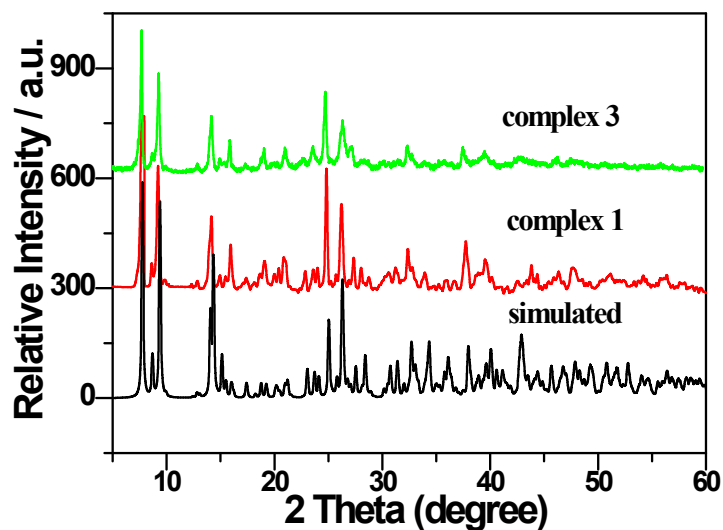


Fig. S1 Powder X-ray diffraction profiles of **1** and **3** together with a simulation from the single crystal data.

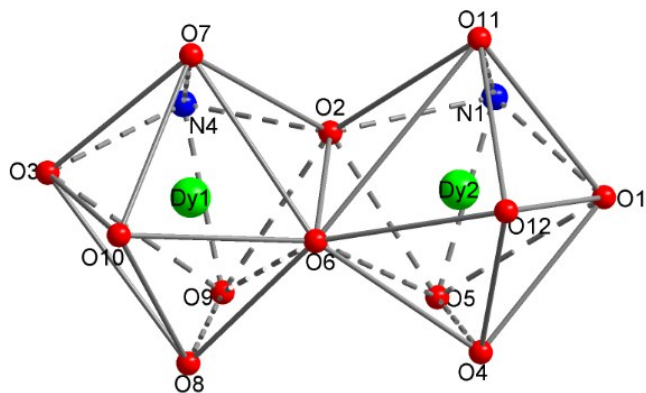


Fig. S2 The coordination polyhedron around two Dy^{3+} ions in complex **1**.

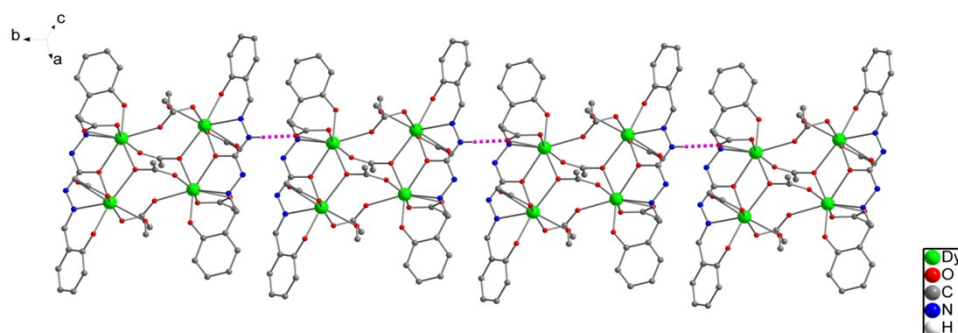


Fig. S3 1D chain of complex **1** constructed by hydrogen bonds.

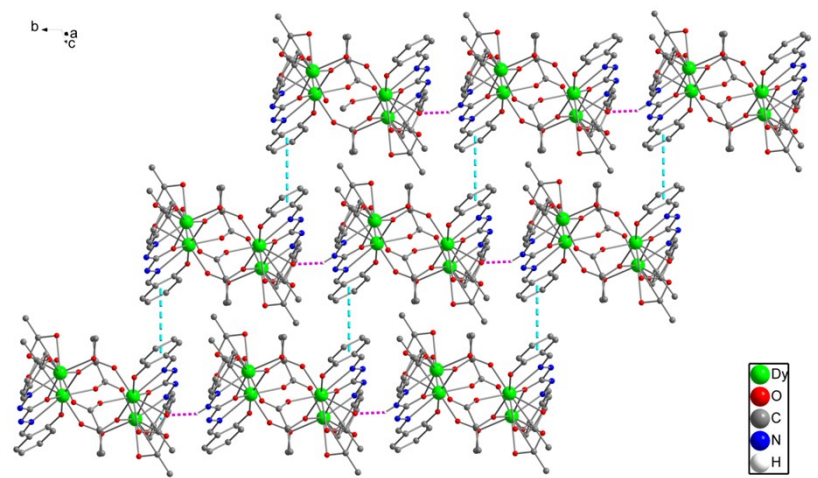


Fig. S4 layer structure of **1** through π - π stackings between interdigitating phenyl and phenyl.

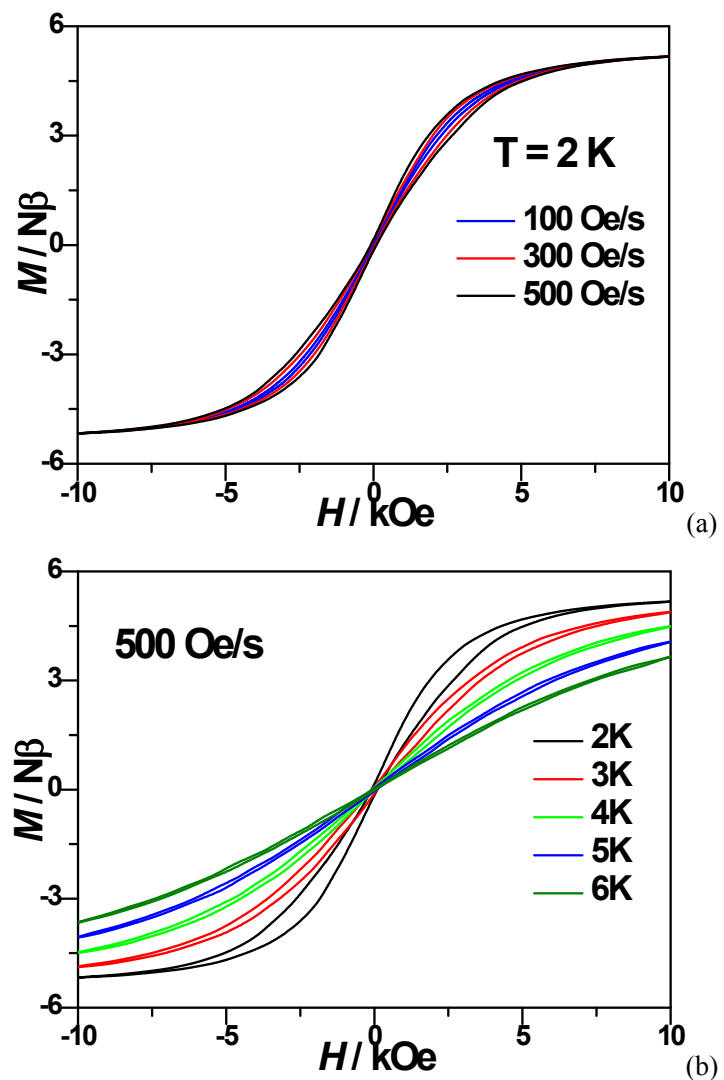


Fig. S5 Hysteresis loop for complex **1** measured at different rates with temperature of 2 K (a) and different temperatures with sweep rates of 500 Oe/s.

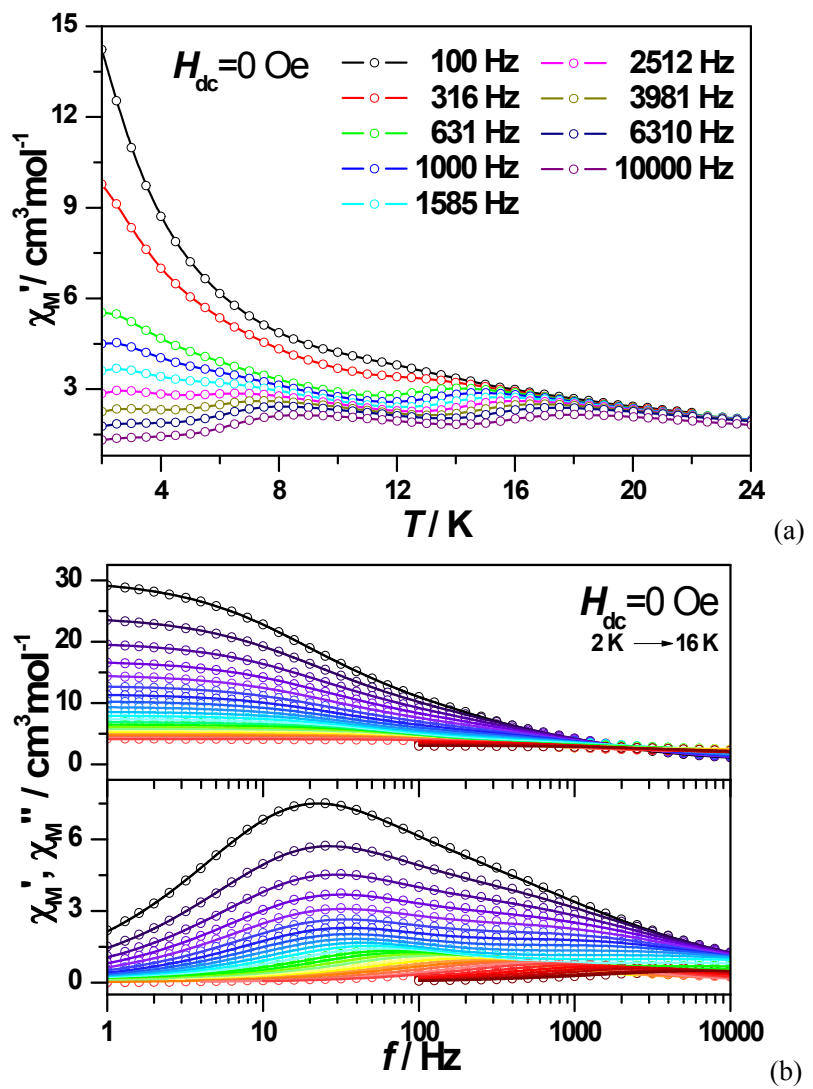


Fig. S6 Temperature dependence of the in-phase ac susceptibility signal (a) and frequency dependence of the in-phase (top) and out-of-phase (bottom) ac susceptibility signal (b) under the zero field for complex **1**.

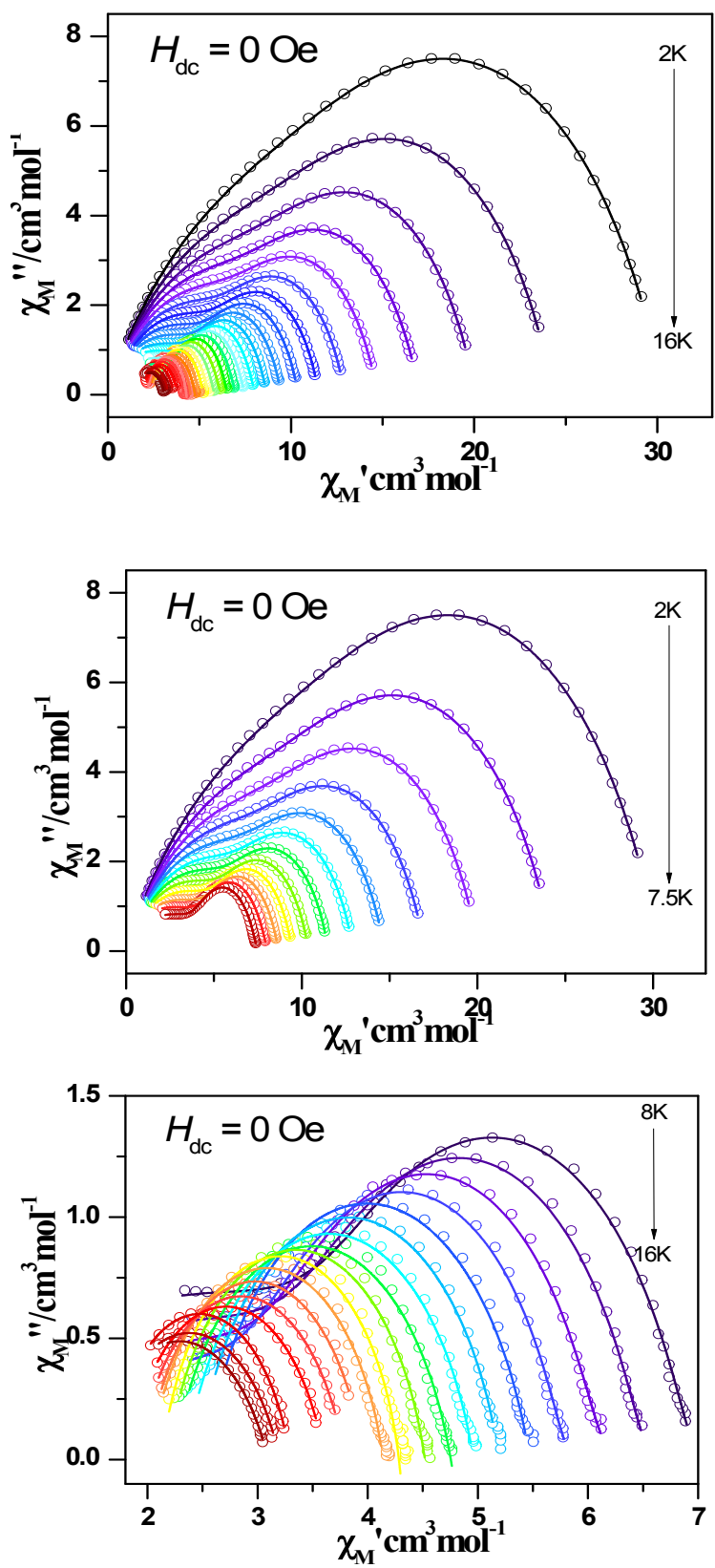


Fig. S7 Cole-cole plots of complex **1** under zero dc field.

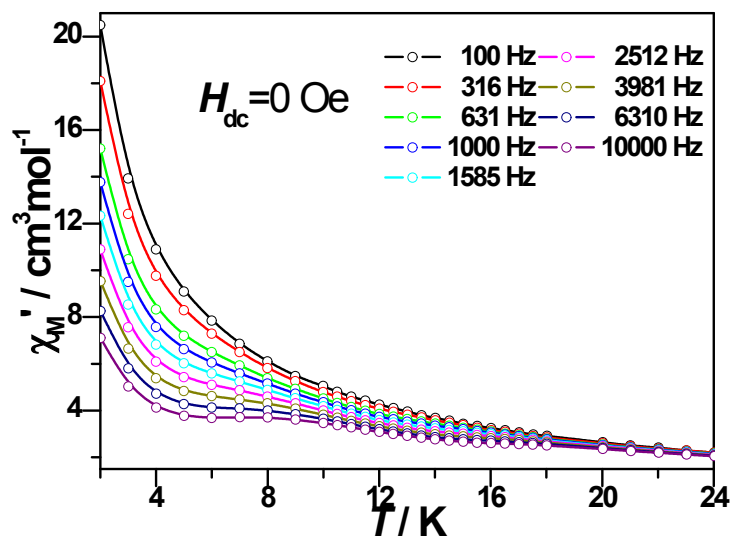


Fig. S8 Temperature dependence of the in-phase ac susceptibility signal under the zero field for complex **3**.

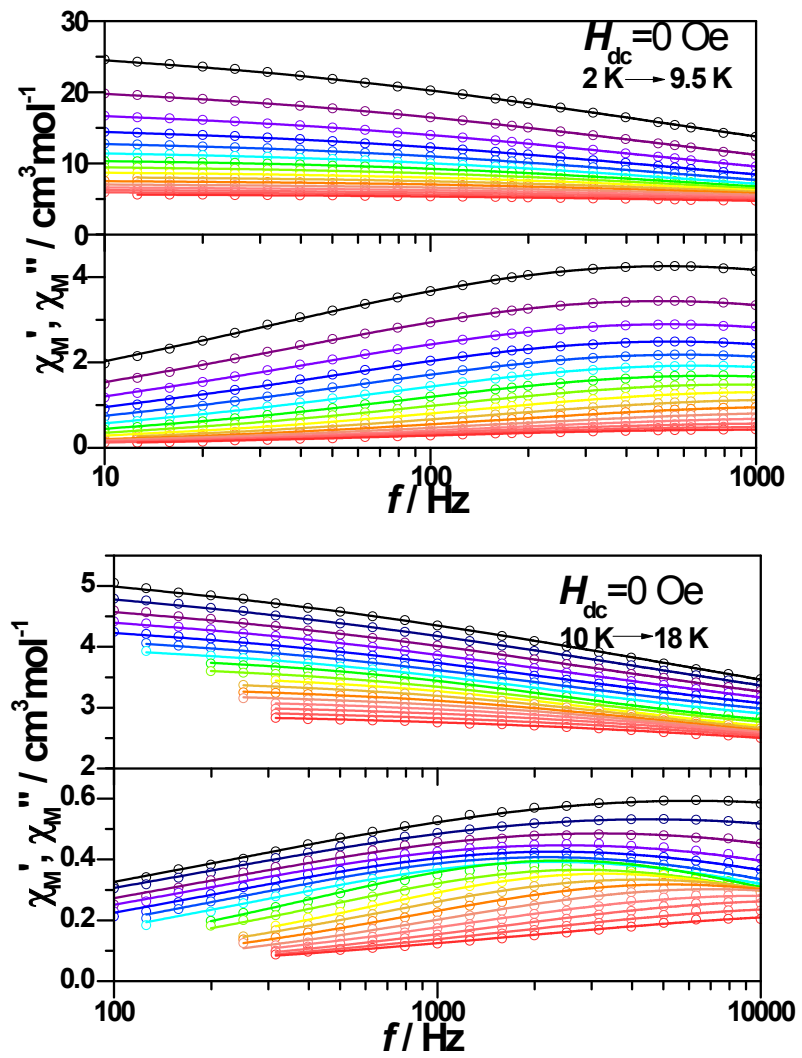


Fig. S9 Frequency dependence of the in-phase (top) and out-of-phase (bottom) ac susceptibility signal under the zero field for complex 3.

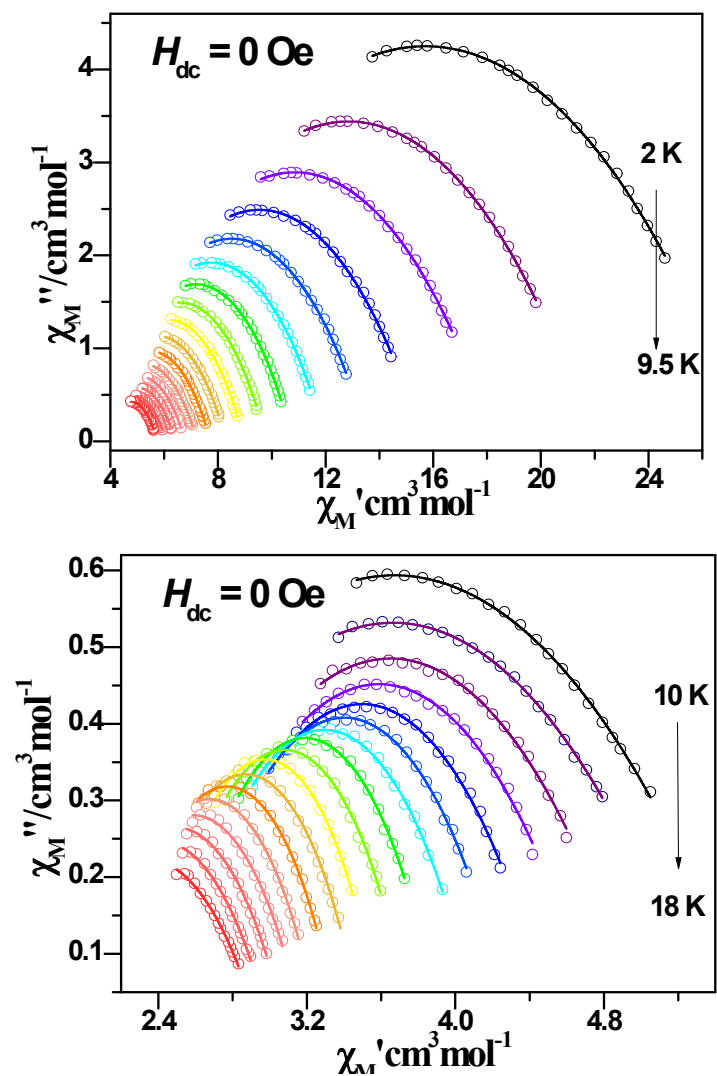


Fig. S10 Cole-cole plots of complex **3** under zero dc field.

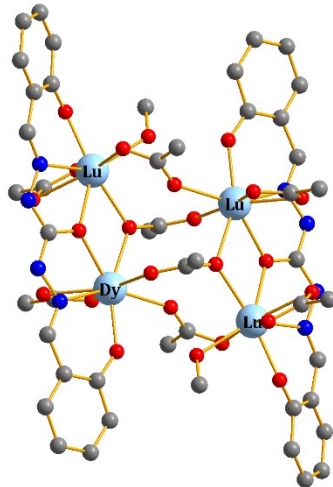


Fig. S11 Calculated model structure of individual Dy1 fragment; H atoms are omitted.

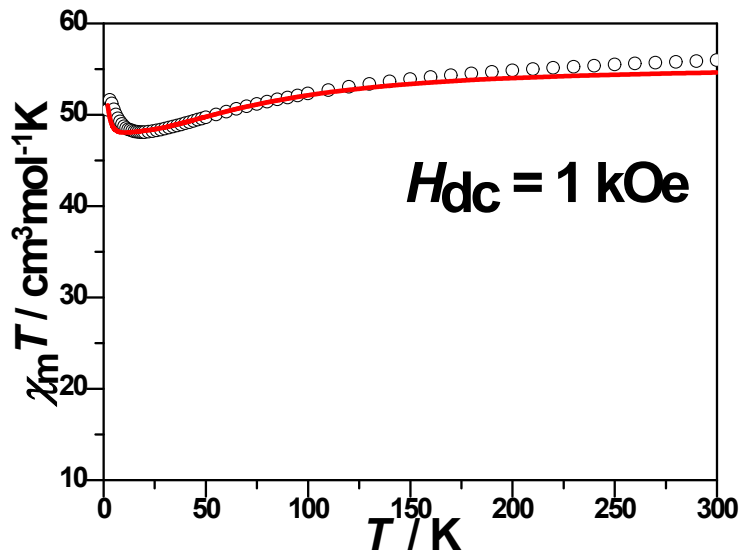


Fig. S12 Temperature dependence of $\chi_M T$ for complex 1. The red solid line is the simulation from ab initio calculation.

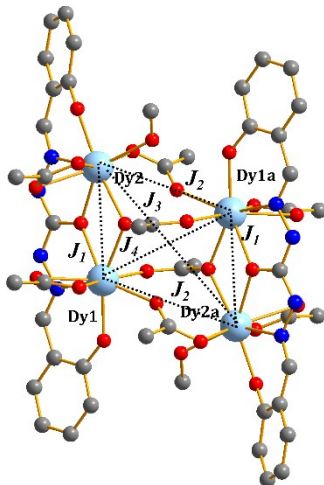


Fig. S13 Four types of J_1 , J_2 , J_3 and J_4 in complex **1**.

References

- 1 (a) F. Aquilante, L. De Vico, N. Ferré, G. Ghigo, P.-Å. Malmqvist, P. Neogrády, T. B. Pedersen, M. Pitonak, M. Reiher, B. O. Roos, L. Serrano-Andrés, M. Urban, V. Veryazov and R. Lindh, *J. Comput. Chem.*, 2010, **31**, 224; (b) V. Veryazov, P.-O. Widmark, L. Serrano-Andres, R. Lindh and B. O. Roos, *Int. J. Quantum Chem.*, 2004, **100**, 626; (c) G. Karlström, R. Lindh, P.-Å. Malmqvist, B. O. Roos, U. Ryde, V. Veryazov, P.-O. Widmark, M. Cossi, B. Schimmelepfennig, P. Neogr'ady and L. Seijo, *Comput. Mater. Sci.*, 2003, **28**, 222.
- 2 (a) L. F. Chibotaru, L. Ungur and A. Soncini, *Angew. Chem. Int. Ed.*, 2008, **47**, 4126; (b) L. Ungur, W. Van den Heuvel and L. F. Chibotaru, *New J. Chem.*, 2009, **33**, 1224; (c) L. F. Chibotaru, L. Ungur, C. Aronica, H. Elmoll, G. Pilet and D. Luneau, *J. Am. Chem. Soc.*, 2008, **130**, 12445.
- 3 Lines, M. E. *J. Chem. Phys.* **1971**, *55*, 2977.
- 4 (a) K. C. Mondal, A. Sundt, Y. H. Lan, G. E. Kostakis, O. Waldmann, L. Ungur, L. F. Chibotaru, C. E. Anson and A. K. Powell, *Angew. Chem. Int. Ed.*, 2012, *51*, 7550; (b) S. K. Langley, D. P. Wielechowski, V. Vieru, N. F. Chilton, B. Moubaraki, B. F. Abrahams, L. F. Chibotaru and K. S. Murray, *Angew. Chem. Int. Ed.*, 2013, **52**, 12014.